MECHANISTIC SEISMIC DAMAGE MODEL FOR REINFORCED CONCRETE

By Young-Ji Park[1] and Alfredo H.-S. Ang,[2] F. ASCE

ABSTRACT: A model for evaluating structural damage in reinforced concrete structures under earthquake ground motions is proposed. Damage is expressed as a linear function of the maximum deformation and the effect of repeated cyclic loading. Available static (monotonic) and dynamic (cyclic) test data were analyzed to evaluate the statistics of the appropriate parameters of the proposed damage model. The uncertainty in the ultimate structural capacity was also examined.

INTRODUCTION

In earthquake-resistant design of reinforced concrete structures, it is generally necessary to permit some degree of damage; otherwise the design would be too costly. In order to implement this philosophy properly, models for assessing structural damage within the context of a random earthquake environment are required. A reinforced concrete structure is weakened or damaged by a combination of stress reversals and high stress excursion. Consequently, any damage criterion should include not only the maximum response, but also the effect of repeated cyclic loadings (4,12).

Current seismic design codes, such as the UBC and SEAOC codes, are based primarily on research results of flexural behavior of reinforced concrete under monotonic loadings (e.g., Refs. 5, 11, and 23). Under monotonic loadings, brittle failure modes such as shear and bond failures can be avoided through careful detailing of the members, and the ultimate flexural capacity can be accurately evaluated (5). However, under repeated cyclic loadings, it is difficult to ensure that such brittle failure modes will not occur.

Küstü and Bouwkamp (21) conducted cyclic loading tests on eight beam-column subassemblages. Extremely brittle shear failure was observed in all of the columns although every column was designed to fail in flexure under a monotonic loading, revealing the inadequacy of design provisions based entirely on results of monotonic tests. A comprehensive research program on the behavior of reinforced concrete under cyclic loadings was conducted in Japan, using approximately three hundred half-scale columns (8). The main variables included the loading history, axial load, shear span ratio, longitudinal steel content, concrete strength, stirrup ratio, and joint details. The results revealed the complex failure mechanism of components under loading reversals. The major findings included the following: (1) A column designed to fail in flexure (under

[1]Grad. Research Asst. of Civ. Engrg., Univ. of Illinois at Urbana-Champaign, Ill. 61801.

[2]Prof. of Civ. Engrg., Univ. of Illinois at Urbana-Champaign, Ill. 61801.

Note.—Discussion open until September 1, 1985. Separate discussions should be submitted for the individual papers in this symposium. To extend the closing date one month, a written request must be filed with the ASCE Manager of Journals. The manuscript for this paper was submitted for review and possible publication on November 15, 1983. This paper is part of the *Journal of Structural Engineering*, Vol. 111, No. 4, April, 1985. ©ASCE, ISSN 0733-9445/85/0004-0722/$01.00. Paper No. 19670.

J. Struct. Eng. 1985.111:722-739.

monotonic loading) tends to fail in shear under repeated cyclic loadings; and (2) when the number of reversals is significantly increased, the members tend to fail through bond at a much lower level of deformation than would be expected under a monotonic loading. An analysis of these tests showed that the error in predicting the ultimate strength is small; however, a significant scatter was observed in the prediction of the deformation capacity and energy absorbing capacity.

The large uncertainty inherent in the prediction of the ultimate structural capacity of reinforced concrete components under repeated cyclic loadings was also observed by Banon et al. (4) and Hwang (16). Structural damage was expressed as a function of the maximum deformation and absorbed hysteretic energy by Banon et al., whereas a simple scaling, in terms of the "energy index," was used by Hwang. Although the results were based on limited data, 29 test specimens in Banon et al. (4) and 34 specimens in Hwang (16), significant scatter was observed.

In the present study, a damage model is developed for expressing the potential damage of reinforced concrete comonents as a function of the maximum deformation and the absorbed hysteretic energy. In developing the necessary damage function, extensive test data were examined. Monotonic and cyclic test data of reinforced concrete beams and columns reported in the U.S. (e.g., Refs. 3, 5, 6, 21, 26, 31) and Japan (e.g., Refs. 8, 14, 15) were used in a systematic regression analysis. The pertinent data were all for rectangular sections reinforced with deformed bars (loaded under a single-axis bending).

Damage Model

Consistent with the dynamic behavior of reinforced concrete described earlier, seismic structural damage is expressed as a linear combination of the damage caused by excessive deformation and that contributed by repeated cyclic loading effect. This may be represented in terms of a damage index

$$D = \frac{\delta_M}{\delta_u} + \frac{\beta}{Q_y \delta_u} \int dE \quad \ldots\ldots (1)$$

$$\text{or} \quad D = \frac{\delta_M}{\delta_u} + \beta \int \left(\frac{\delta}{\delta_u}\right)^{\alpha} \frac{dE}{E_c(\delta)} \quad \ldots\ldots (2)$$

in which δ_M = maximum deformation under earthquake; δ_u = ultimate deformation under monotonic loading; Q_y = calculated yield strength (if the maximum strength, Q_u, is smaller than Q_y, Q_y is replaced by Q_u); $E_c(\delta)$ = hysteretic energy per loading cycle at deformation, δ; dE = incremental absorbed hysteretic energy; α, β = non-negative parameters. Under elastic response, the value of D should theoretically be zero. However, Eqs. 1 or 2 will give nonzero but negligibly small values of D in the elastic range.

Values of the damage index, D, are such that $D \geq 1.0$ signifies complete collapse or total damage. Structural damage, therefore, is a function of the responses δ_M and dE that are dependent on the loading history, whereas the parameters α, β, δ_u, Q_y, and $E_c(\delta)$, are independent of the loading history. In Eq. 2, the cyclic loading effect at different de-

formation levels is taken into account, whereas in Eq. 1 such effect is assumed to be uniform at all deformation levels.

Determination of Model Parameters

The damage model proposed in Eq. 1 contains the three parameters δ_u, Q_y, and β. In Eq. 2, two additional parameters, α and $E_c(\delta)$, are also required. In this paper, Eq. 1 is emphasized by virtue of its simplicity. The required parameters are evaluated on the basis of available experimental data as described in this section.

Determination of δ_u.—When brittle shear failure is of no concern, such as for very slender beams and columns, the ultimate deformation can be evaluated from the stress-strain relationship of the material. However, as mentioned earlier, components may fail in shear under repeated cyclic loadings even though a flexural failure is expected under monotonic loadings. In other words, all possible failure modes should be taken into account in evaluating δ_u when repeated cyclic loadings are involved.

To date, there appears to be no reliable method for determining the ultimate deformation of reinforced concrete components, especially when shear deformation and bond slippage may be dominant. Even highly sophisticated finite element analysis cannot trace the deformation behavior up to the ultimate stage because of uncertainties in the dowel action, shear crackings, bond deterioration, three-dimensional stress concentration, etc. In this light, a simple empirical relation is developed for determining δ_u using available monotonically loaded test data.

Because the yield deformation, δ_y, can be predicted with good accuracy, a practical means to determine the ultimate deformation may be to amplify this with the ductility factor, μ_u; namely

$$\delta_u = \mu_u \delta_y \quad \ldots\ldots (3)$$

The values μ_u and δ_y may be determined independently. Yielding of a reinforced concrete component may be defined as the first yielding in the tension reinforcement, or when the extreme fiber compressive strain in the concrete exceeds 1.5 times the crushing strain, ϵ_o.

The yield deformation can be regarded as composed of the flexural component, δ_f, the deformation due to bond slippage of the reinforcing bar from its anchorage, δ_b, the inelastic shear deformation, δ_s, and the elastic shear deformation, δ_e; i.e.

$$\delta_y = \delta_f + \delta_b + \delta_s + \delta_e \quad \ldots\ldots (4)$$

in which δ_e may be evaluated by the conventional elastic beam theory. Three of the components in Eq. 4 can be evaluated with reference to Fig. 1 as follows.

Flexural Deformation.—It is well-known that the yield curvature can be reasonably determined by the plane section assumption, and the curvature distribution along a member is approximately linear (5). By assuming that the concrete in compression remains elastic up to yielding of the tension reinforcement, the yield curvature for beams can be expressed as follows (28)

$$\phi_y' = \frac{\epsilon_y}{(1-k)d} \quad \ldots\ldots (5)$$

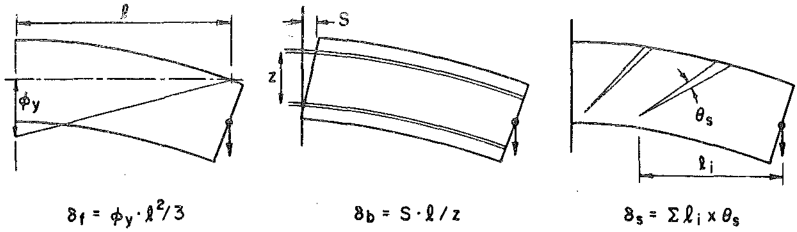

FIG. 1.—Three Components of Inelastic Deformation at Yielding

in which $k = [(\rho + \rho')^2\, 1/4\alpha_y^2 + (\rho + \beta_c\rho')\, 1/\alpha_y]^{1/2} - (\rho + \rho')\, 1/2\alpha_y$; $\rho = a_t\sigma_y/bdf_c'$; $\rho' = a_c\sigma_y/bdf_c'$; $\alpha_y = \epsilon_y/\epsilon_o$; and $\beta_c = d_c/d$. See Figs. 2 and 3 for the definitions of the parameters. Because of the inelasticity of concrete and the effect of axial forces, Eq. 5 tends to underestimate the actual curvature. Based on results of iterative analyses (e.g., Ref. 2), the following improvement is proposed:

$$\phi_y = \left\{1.05 + \left(\frac{0.45}{0.84 + 2\rho' - \rho} - 0.05\right)\frac{n_o}{0.3}\right\}\phi_y' \quad \text{(6)}$$

in which $n_o = N/(f_c'bd)$; and N = the axial force.

Deformation Due to Bond Slippage.—With the assumption that the deformation of concrete in the anchorage is negligible, the following relation can be obtained between the bond stress, τ, and bond slippage, S

$$\tau = \frac{AE_S}{\psi}\frac{d^2S}{d^2x} \quad \text{(7)}$$

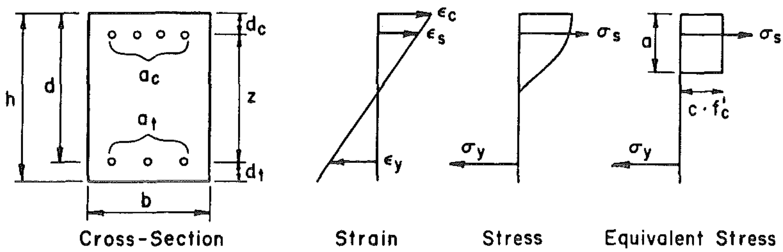

FIG. 2.—Cross Section of Member

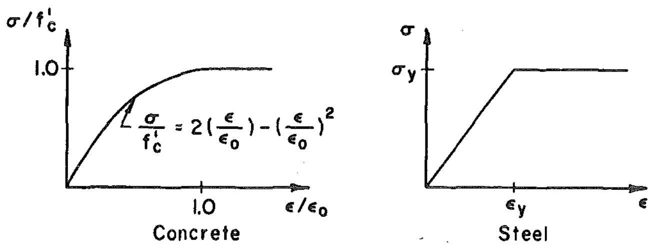

FIG. 3.—Stress and Strain Relation of Material

in which A = area of the reinforcing bars; ψ = perimeter of the reinforcing bars; and E_S = modulus of elasticity of steel. Using the idealized bond slippage relation shown in Fig. 4, the stress in the reinforcing bar at the face of the anchorage, σ_o, may be expressed as a simple function of the normalized slippage

$$\sigma_o = \sqrt{6E_S}\,\lambda^{1/6}\tau_M^{1/2}S_n^{2/3} \simeq 225.5\,\tau_M^{1/2}S_n^{2/3} \quad \text{(in ksi)} \ldots\ldots\ldots\ldots\ldots\ldots (8)$$

in which $\lambda = S_o/D \simeq 1/40$; and $S_n = S/D$, the normalized slippage. The validity of Eq. 8 had been examined with available pullout test data (10), assuming $\tau_M = 1.5$ ksi for the bottom bars, and $\tau_M = 0.9$ ksi for the top bars. When the anchorage length is longer than 10 D, Eq. 8 agrees well with experimental results as shown in Fig. 5. Results of other pullout tests (7,17,20,22,24) are also shown in Fig. 6. On the basis of the preceding experimental results, it can be observed that the bond slippage is largely a function of the degree of compactness of the concrete, and independent of the concrete strength. For the purpose of determining the deformation due to bond slippage, a mean value of $\tau_M = 1.2$ ksi may be assumed if the degree of compactness is not specified.

Inelastic Shear Deformation.—The shear deformation, δ_s, may be obtained by subtracting the calculated δ_f, δ_b, and δ_e from the measured yield deformation, δ_y. The ratio of the shear deformation to the flexural deformation as a function of the shear span ratio is shown in Fig. 7 for 244 beams and columns in which yielding of the tension reinforcement is clearly recorded. In slender beams and columns, the shear deformation is not prominent; however, as the shear span ratio approaches unity (i.e., $l/d \rightarrow 1.0$), the shear deformation becomes dominant.

It is well-known that the bond stress and stirrup ratio also affect the shear deformation. Available experimental results (e.g., Ref. 8) indicate that as the stirrup ratio is increased to about 1%, the shear deformation generally decreases; however, higher stirrup ratios do not always insure decreasing shear deformations. Fig. 9 shows a well-known bond failure mechanism. As the ribs of the longitudinal reinforcement bear against the surrounding concrete, conical micro cracks are formed around the bar with an inclined angle of about 45° (13). The presence of a stirrup will reduce the bearing stress from being transmitted to the surrounding concrete. Assuming that the shaded part of the longitudinal bar (see Fig. 9) is not effective for bond, the effective average bond stress, τ_B, is

$$\tau_B = \frac{\Delta T}{\psi(l - 1.71\,nd)} \ldots\ldots\ldots\ldots\ldots\ldots\ldots\ldots\ldots\ldots\ldots\ldots\ldots\ldots (9)$$

in which ΔT = difference of the forces in the reinforcement between both ends of a member calculated by flexural analysis; ψ = perimeter of the longitudinal reinforcement; l = length of member; n = number of pairs of stirrups; and d = diameter of stirrups. Therefore, according to Eq. 9, an excessive number of stirrups has the effect of reducing the effective bond length, and thus increasing the bond stress. Fig. 8 would appear to suggest a weak positive correlation between the shear deformation and the normalized effective average bond stress, $\tau_B/\sqrt{f'_c}$. As seen in both Figs. 7 and 8, the scatter in the shear deformation is high if δ_s is expressed as a function of a single parameter. This scatter can be

J. Struct. Eng. 1985.111:722-739.

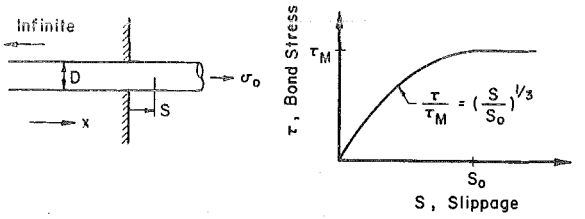

FIG. 4.—Bond Slippage at Anchorage

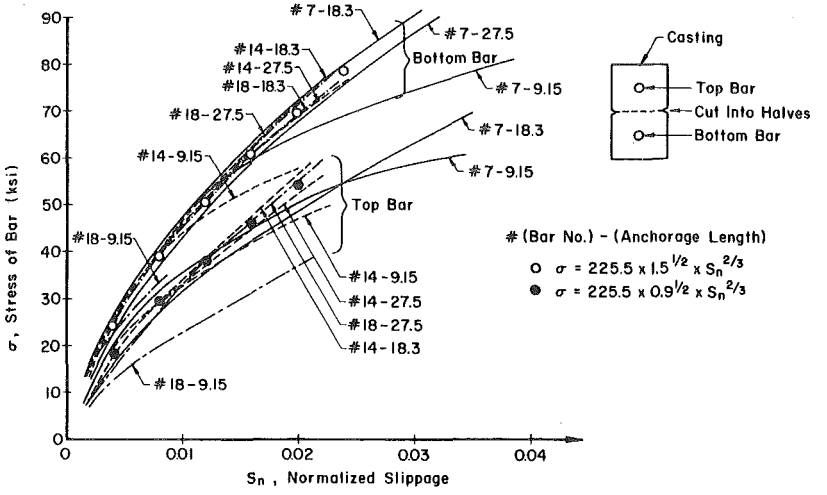

FIG. 5.—Pullout Tests by Ferguson

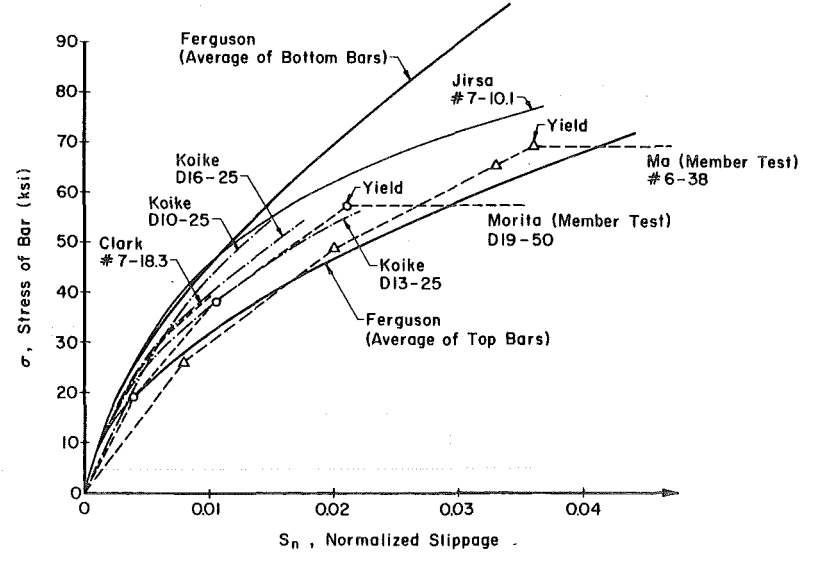

FIG. 6.—Pullout Tests by Several Researchers

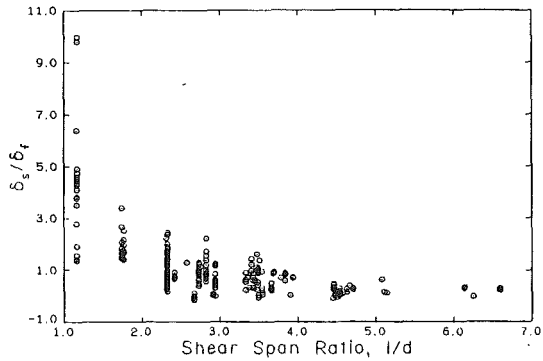

FIG. 7.—Effect of Shear Span Ration on Shear Deformation

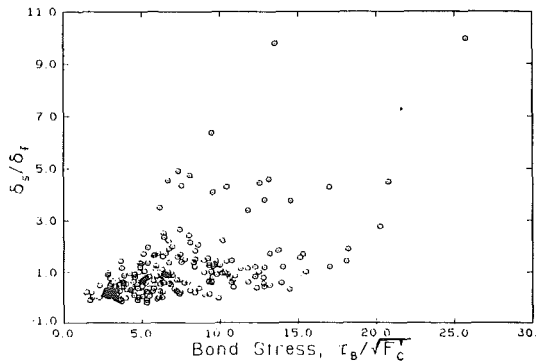

FIG. 8.—Effect of Bond Stress on Shear Deformation

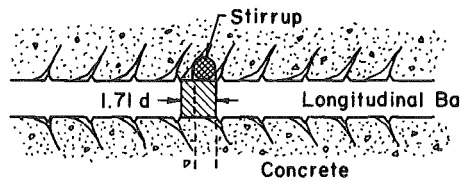

FIG. 9.—Bond Failure Mechanism

reduced by expressing δ_S as a function of several parameters, namely l/d, τ_B, and p_w (stirrup ratio).

An idealized shear cracking model may be assumed. Every shear crack in a member is assumed to be inclined at 45° as shown in Fig. 10 with an identical shear rotation, θ_s. Then the shear deformation of a cantilever is

$$\delta_s = \Sigma l_i \times \theta_s \quad \ldots\ldots (10)$$

in which l_i = the arm length measured from the end of the shear crack. According to (27), the shear cracking load, Q_c, is

$$Q_c = \sqrt{f'_c}\, bd + \frac{M_c}{\left(l - \frac{d}{2}\right)} \quad \text{..... (11)}$$

in which M_c = the flexural cracking moment. Eq. 11 may be modified by assuming the length of a "no shear crack zone" to be l', with an occurrence rate of $p = 1/Z$ (see Fig. 10). Then the mean shear deformation is

$$E[\delta_s] = E[\Sigma l_i] \times \theta_s = \left(l + \frac{l^2 - l'^2}{2Z}\right)\theta_s \quad \text{..... (12)}$$

in which $l' = M_c/(Q_c - \sqrt{f'_c}\, bd) + Z$. Using Eq. 12, the shear rotations, θ_s, were evaluated for the 244 test beams and columns. Based on the calculated results, the following is proposed:

$$\theta_s = \frac{0.2}{\left(\frac{l}{d}\right) - 0.5}, \quad \text{as a percentage; for } u < 5 \text{ or } \frac{l}{d} > 4; \quad \text{..... (13a)}$$

$$= \frac{0.2}{\left(\frac{l}{d}\right) - 0.5}[1 + 0.27(u - 5)]; \quad \text{for } u > 5 \text{ and } 2.5 < \frac{l}{d} < 4; \quad \text{... (13b)}$$

$$= \frac{0.2}{\left(\frac{l}{d}\right) - 0.5}\left[1 + 0.185\frac{u - 5}{\sqrt{p_w} - 0.4}\right]; \quad \text{for } u > 5 \text{ and } \frac{l}{d} < 2.5 \quad \text{(13c)}$$

in which l/d = shear span ratio (replaced by 1.5 if $l/d < 1.5$); p_w = stirrup ratio, as a percentage (replaced by 0.2% if $p_w < 0.2\%$); and $u = \tau_B/\sqrt{f'_c}$.

The total yield deformation, therefore, can be calculated with Eq. 4. A comparison of the calculated and normalized experimental yield deformation is shown in Fig. 11.

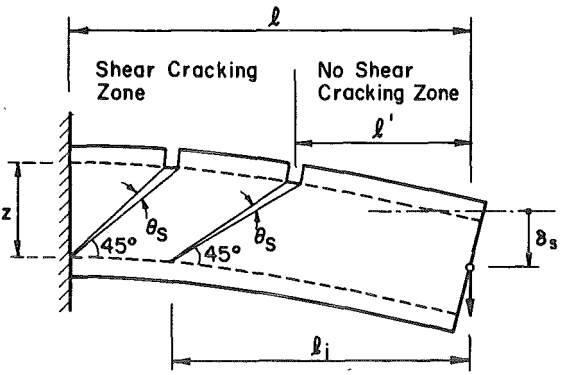

FIG. 10.—Shear Cracking Model

Ultimate Ductility Factor.—Using Eq. 3, the ultimate ductility factors, μ_u, were calculated for 142 monotonically loaded beams and columns.

In order to clarify the definition of the "ultimate state," the test specimens were divided into four categories according to their ultimate failure mode, as defined in Fig. 12.

For a sudden failure, in which a member loses its load-carrying capacity suddenly, there is no difficulty in identifying the failure point. Buckling of the compression reinforcement or fracture of the tension or web reinforcement usually show this type of failure. For a gradual failure, in which a member loses its strength continuously, the failure point is identified on the load-deformation curve when the strength drop exceeds a certain percentage of its maximum strength.

Analyses of the ultimate ductility factors for the test specimens showed a strong correlation with the flexural and shear deformations, whereas there is virtually no correlation with the bond slippage. After examining several mathematical formulations, the following deformation parameter was found to correlate well with μ_u:

$$\epsilon_p = 0.5\,\epsilon_b + 0.5\sqrt{\epsilon_b^2 + \theta_s^2} \quad (14)$$

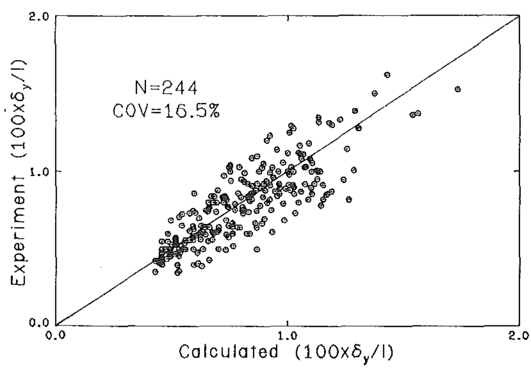

FIG. 11.—Yield Deformation

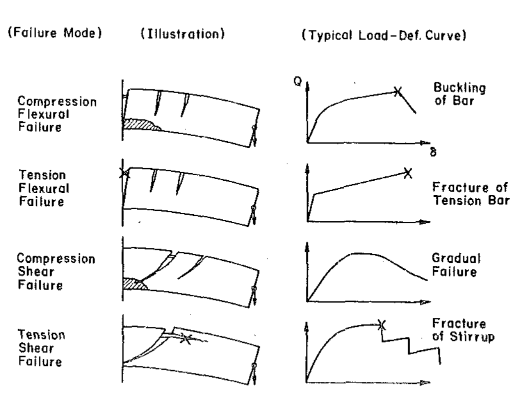

FIG. 12.—Ultimate Failure Mode

J. Struct. Eng. 1985.111:722-739.

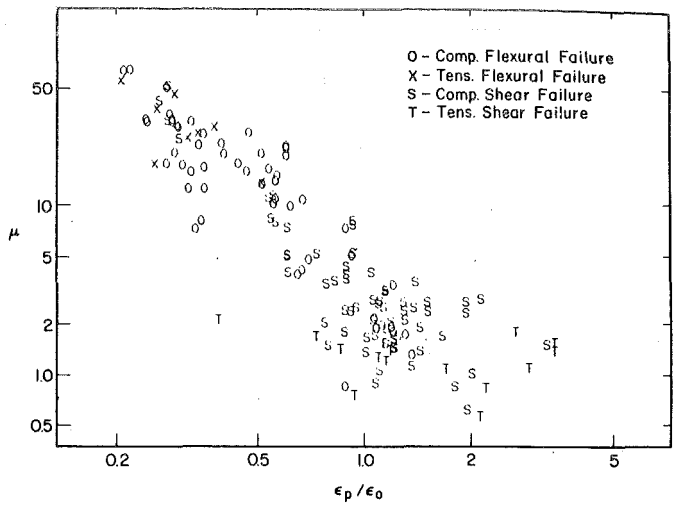

FIG. 13.—Ultimate Ductility Factor-Failure Mode

in which ϵ_p = principal strain; ϵ_b = flexural concrete strain at the location of the compression bar calculated using Eq. 6; and θ_s = shear rotation of Eq. 13. Fig. 13 shows the plot between the principal strain normalized by ϵ_o and the ultimate ductility factor. The correlation between μ_u and ϵ_p/ϵ_o is maximized when the strength drop (for gradually failing members) is assumed to be about 10% of the maximum strength. However, the strength drop at the failure point is defined as 20% of the maximum strength in this study, because the majority of the tests to ultimate col-

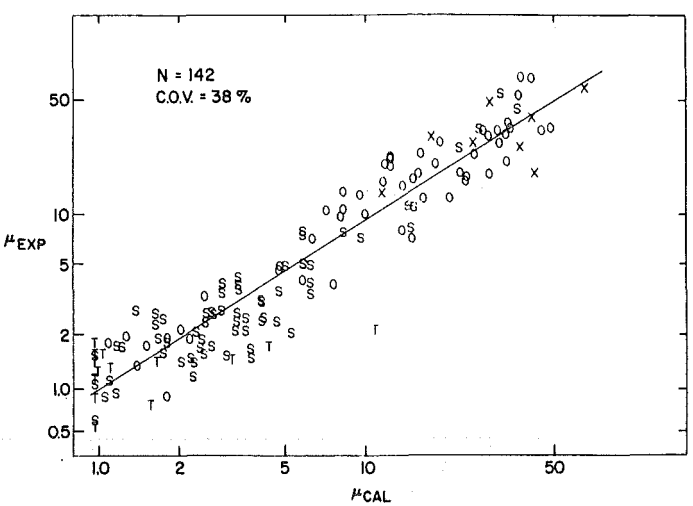

FIG. 14.—Prediction Error in Ultimate Ductility Factor

lapse indicated that total repair is generally needed beyond this point (e.g., Ref. 8).

From Fig. 13, it can be observed that the ultimate ductility factor is independent of the failure mode, indicating the validity of Eq. 14. It was also observed that a positive correlation exists between μ_u and the confinement ratio, ρ_w, which is defined as the volumetric ratio of stirrup to the core concrete. Based on these observations, the following is proposed for the ultimate ductility factor, μ_u:

$$\mu_u = \left(\frac{\epsilon_p}{\epsilon_o}\right)^{0.218\rho_w - 2.15} \exp(0.654\,\rho_w + 0.38) \quad \text{..... (15)}$$

in which ρ_w = the confinement ratio as a percentage (replaced by 2% if $\rho_w > 2\%$), and μ_u is replaced by 1.0 if $\mu_u < 1.0$.

Fig. 14 shows the correlation between the calculated (i.e., Eq. 15) and experimental ultimate ductility factors. The applicable range of the preceding empirical equation is: $1.0 < l/d < 7.0$; $0 \le \rho_w \le 2.0$; $0.05 \le \rho < 0.5$; $0 \le n_o \le 0.55$; and 2.5 ksi $\le f'_c \le$ 5.0 ksi. The scatter around Eq. 15, as shown in Fig. 14, includes the scatter in the predicted value of δ_y.

Determination of β.—The effect of cyclic loading on structural damage is represented by the parameter β in Eqs. 1 and 2. The absorbed hysteretic energy (excluding potential energy) is integrated up to the failure point for a large set (261) of cyclic test data of beams and columns. These experimental data were carefully selected from a larger set of test specimens; only those in which an abrupt failure is clearly observed or gradual failure can be identified on the envelope curve were included.

Using Eq. 1 or 2, the load-deformation curve for each test is traced up to the failure point. Then, at the point of failure, $D = 1.0$, the corresponding value of β is evaluated. Based on the calculated β values, a negative correlation was observed between β and the confinement ratio, ρ_w, and also weak positive correlations were observed between β and the shear span ratio, l/d, longitudinal steel ratio, p_t, and axial stress, n_o.

Through trial and error, the minimum-variance values of β for Eq. 1 are determined in such a way that the standard deviation of D is minimized and the mean value of D is close to unity. In a similar manner, and with $\alpha = 0.6$, the corresponding optimal values of β for Eq. 2 are also obtained. The results yielded the following:

$$\text{for Eq. 1:} \quad \beta = \left(-0.447 + 0.073\frac{l}{d} + 0.24\,n_o + 0.314\,p_t\right) \times 0.7^{\rho_w} \text{..... (16)}$$

$$\text{for Eq. 2:} \quad \beta = \left(-0.165 + 0.0315\frac{l}{d} + 0.131\,p_t\right) \times 0.84^{\rho_w} \text{ ..... (17)}$$

in which l/d = shear span ratio (replaced by 1.7 if $l/d < 1.7$); n_o = normalized axial stress (replaced by 0.2 if $n_o < 0.2$); p_t = longitudinal steel ratio as a percentage (replaced by 0.75% if $p_t < 0.75\%$); and ρ_w = confinement ratio. A large scatter can be observed between the calculated (Eq. 1 or 2) and experimental results of β as shown in Figs. 15 and 16. The applicable range of the above empirical equations, Eqs. 16 and 17,

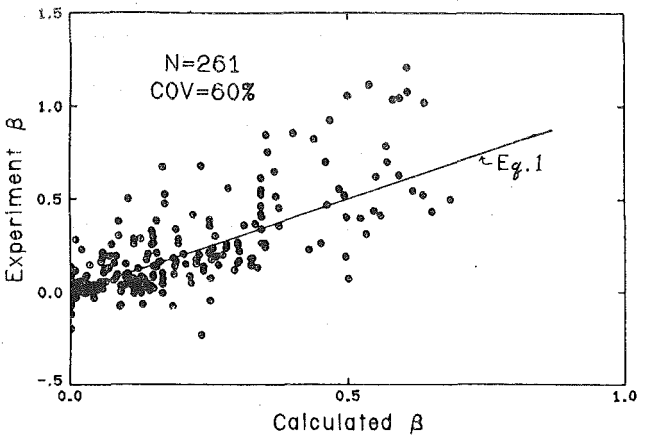

FIG. 15.—β Value for Eq. 1

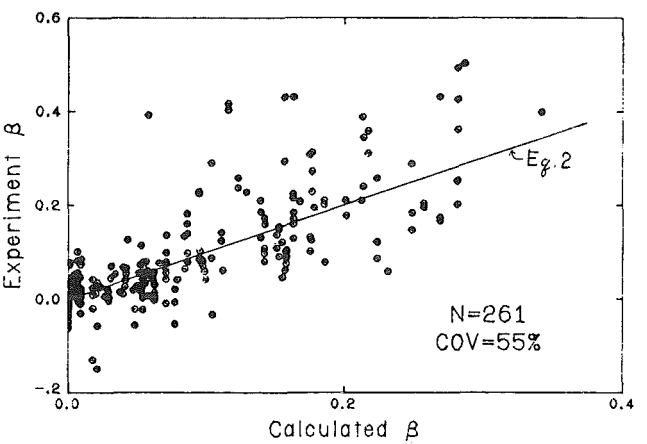

FIG. 16.—β Value for Eq. 2

is $1.0 < l/d < 6.6$; $0.2 < \rho_w < 2.0$; $0.04 < \rho < 0.45$; $0 \leq n_o < 0.52$; and 2.3 ksi $< f'_c <$ 6.0 ksi.

Determination of Q_y and Q_u.—The method for evaluating the yield strength, Q_y, may be found in standard text books (e.g., Ref. 28). For the maximum strength, Q_u, of reinforced concrete beams and columns subjected to reversed loadings the following is proposed based on the analysis of experimental data.

$$Q_u = (1.24 - 0.15\,\rho - 0.5\,n_o)Q_y \quad \ldots\ldots (18)$$

in which ρ and n_o are as defined in Eqs. 5 and 6. The scatter associated with Eq. 18 is relatively small; c.o.v. = 12%.

Determination of $E_c(\delta)$.—$E_c(\delta)$ is the hysteretic energy per cycle at deformation δ. About 800 hysteresis loops from 261 cyclic test data were

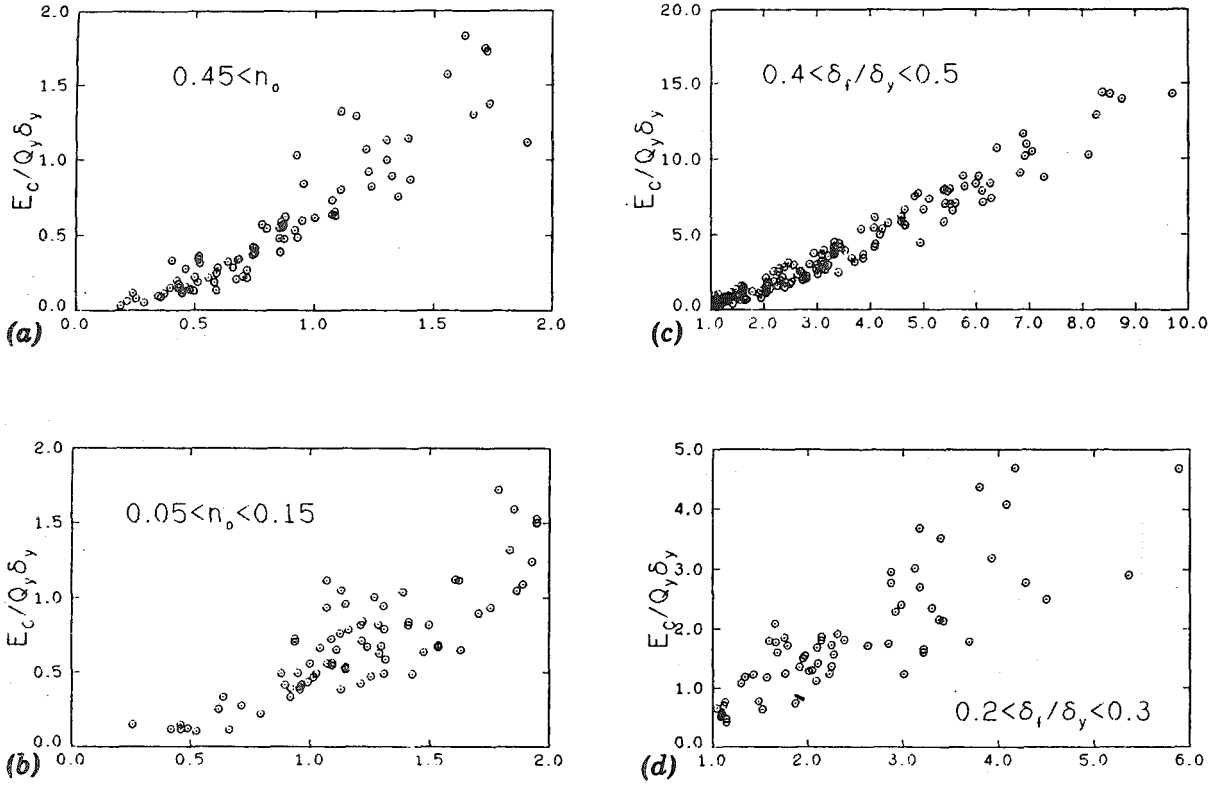

FIG. 17.—Experimental Data of Hysteretic Energy: (*a*) 0.45 < n_o; (*b*) 0.05 < n_o < 0.15; (*c*) 0.4 < δ_f/δ_y < 0.5; (*d*) 0.2 < δ_f/δ_y < 0.3

J. Struct. Eng. 1985.111:722-739.

evaluated to determine this parameter. In this evaluation, the areas of those hystereses with closed loops were used. E_c (normalized by $Q_y\delta_y$) is plotted against the ductility factor, μ, in Fig. 17. On this basis, the relationship between the hysteretic energy and ductility factor may be approximated by a bilinear curve with a transition point at around $\mu = 1.5$.

Figs. 17(*a–b*) show the normalized hysteretic energy at relatively small deformations. As the axial force increases, the normalized hysteretic energy tends to increase slightly. However, considering that there is a significant scatter in the plot, the effect of axial force may be neglected. Linear regression of the experimental data for $\mu < 1.5$ yields the following:

$$E_c(\mu) = Q_y\delta_y(0.77\mu - 0.22); \quad \mu < 1.5 \quad \ldots\ldots (19)$$

Figs. 17(*c–d*) show a part of the data for the normalized hysteretic energy for $\mu > 1.0$. In this range of μ, the ratio of the flexural deformation to the total yield deformation, δ_f/δ_y, controls the energy absorbing characteristics. As the ratio δ_f/δ_y increases, the rate of increase of the absorbed energy also increases [see Figs. 17(*c–d*)]. At low values of δ_f/δ_y, the scatter of the data increases considerably as shown in Fig. 17(*d*). In this range, the effects of δ_s and δ_b are dominant. Linear regression of the data for $\mu \geq 1.5$ yields the following:

$$E_c(\mu) = Q_y\delta_y\left\{\left(0.5 + 2.34\frac{\delta_f}{\delta_y}\right)(\mu - 1) + \left(0.7 - 1.54\frac{\delta_f}{\delta_y}\right)\right\};$$

$$\mu \geq 1.5 \quad \ldots\ldots (20)$$

In calculating the ratio, δ_f/δ_y, Eqs. 4 and 6 may be used. Eqs. 19 and 20 may also be used for properly modeling the hysteresis behavior of reinforced concrete components under dynamic loadings. The average c.o.v.'s about Eqs. 19 and 20 are both approximately 25%.

Damage Index Statistics

With the appropriate model parameters evaluated empirically herein, damage indices for each of the 142 monotonic and 261 cyclic test specimens were evaluated with Eqs. 1 and 2 at the respective failure point. The results obtained with Eqs. 1 and 2 are plotted on lognormal probability papers in Figs. 18 and 19, respectively. These show that the damage index, D, is reasonably lognormally distributed with the respective standard deviation indicated in Figs. 18 and 19. The standard deviation associated with Eq. 2 is slightly lower than that of Eq. 1. However, by virtue of its simplicity, Eq. 1 is preferred for seismic damage assessment of reinforced concrete structures.

The high degree of scatter (or uncertainty) in the damage capacity of reinforced concrete components, (c.o.v. of $D \simeq 0.5$) indicated in Figs. 18 and 19 is in agreement with results of similar previous studies, e.g., Refs. 4 and 16. It may be emphasized that such high uncertainty (c.o.v. $\simeq 0.5$) should be expected, as the capacity under repeated cyclic loadings is much less predictable than under monotonic loadings. Moreover, for

J. Struct. Eng. 1985.111:722-739.

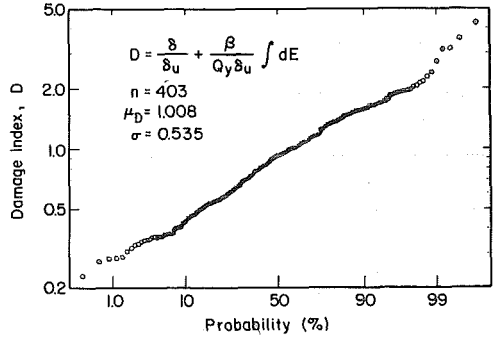

FIG. 18.—Damage Index, D, of Eq. 1 Plotted on Lognormal Probability Paper

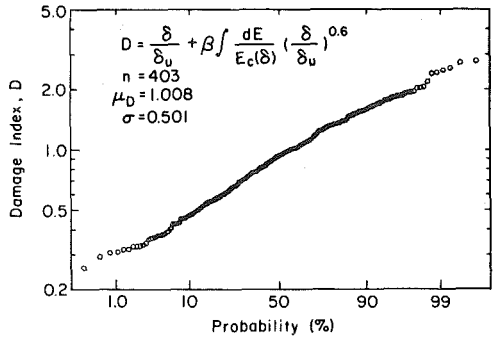

FIG. 19.—Damage Index, D, of Eq. 2 Plotted on Lognormal Probability Paper

some of the parameters, e.g., the ductility factor, μ, the test data show inherently high degree of scatter.

Summary and Conclusions

A seismic damage model for reinforced concrete members is proposed. The model is based on the premise that the total damage from earthquake motions is composed of the damage caused by the maximum structural deformation and the absorbed hysteretic energy. Damage is measured in terms of an index, D, with values $D \geq 1.0$ representing total collapse.

Available monotonic and cyclic test data were analyzed to evaluate the statistics of the appropriate parameters of the proposed damage model. The lognormal distribution was determined to be appropriate for the damage index of reinforced concrete components.

Values of the damage index should be calibrated with observed seismic damage of structures; this calibration is described in Ref. 29.

Acknowledgments

The study was supported by the National Science Foundation under Grant No. CEE 82-13729 of the Division of Civil and Environmental Engineering. This support is gratefully acknowledged.

Appendix I.—References

1. Ang, A. H-S., and Tang, W. H., *Probability Concepts in Engineering Planning and Design*, Vol. 1, John Wiley and Sons, Inc., New York, N.Y., 1975.
2. Aoyama, H., "Moment-Curvature Characteristics of Reinforced Concrete Members Subjected to Axial Load and Reversal of Bending," *Proceedings, International Symposium on the Flexural Mechanics of Reinforced Concrete*, ASCE-ACI, Miami, Fla., Nov., 1964.
3. Atalay, M. B., and Penzien, J., "The Seismic Behavior of Critical Regions of Reinforced Concrete Components as Influenced by Moment, Shear and Axial Force," University of California at Berkeley, EERC, *Report No. 75-19*, Berkeley, Calif., Dec., 1975.
4. Banon, H., Biggs, J. M., and Irvine, H. M., "Prediction of Seismic Damage in Reinforced Concrete Frames," Seismic Behavior and Design of Buildings, *Report No. 3*, MIT, Cambridge, Mass., May, 1980.
5. Burns, N. H., and Siess, C. P., "Load-Deformation Characteristics of Beam-Column Connections in Reinforced Concrete," Civil Engineering Studies, *Structural Research Series No. 234*, University of Illinois, Urbana, Ill., Jan., 1962.
6. Celebi, M., and Penzien, J., "Experimental Investigation into the Seismic Behavior of Critical Regions of Reinforced Concrete Components as Influenced by Moment and Shear," University of California at Berkeley, EERC, *Report No. 73-4*, Berkeley, Calif., Jan., 1973.
7. Clark, A. P., "Comparative Bond Efficiency of Deformed Concrete Reinforcing Bars," *Journal of ACI*, Dec., 1946.
8. "The Comprehensive Research for the Prevention of Failure in Short Reinforced Concrete Columns," Short Column Committee, *Series 1–62, (in Japanese)*, Annual Conference of AIJ, 1973–1977.
9. Ferguson, P. M., and Thompson, J. N., "Development Length of High Strength Reinforcing Bars in Bond," *Journal of ACI*, Aug., 1962.
10. Ferguson, P. M., Breen, J. E., and Thompson, J. N., "Pullout Test on High Strength Reinforcing Bars," *Journal of ACI*, Aug., 1965.
11. Gaston, J. R., Siess, C. P., and Newmark, N. M., "An Investigation of the Load-Deformation Characteristics of Reinforced Concrete Beams Up to the Point of Failure," Civil Engineering Studies, *Structural Research Series No. 40*, University of Illinois, Urbana, Ill., Dec., 1952.
12. Gosain, N. K., Brown, R. H., and Kirsa, J. O., "Shear Requirements for Load Reversals on RC Members," *Journal of the Structural Engineering Division*, ASCE, Vol. 103, No. ST7, July, 1977.
13. Goto, Y., "Cracks Forced in Concrete Around Deformed Tension Bars," *ACI Journal*, Apr., 1971.
14. Hirosawa, M., Goto, T., and Fujiki, Y., *Past Experimental Results on Reinforced Concrete Columns*, in Japanese, Building Research Institute, Ministry of Construction of Japan, Feb., 1973.
15. Hirosawa, M., *Past Experimental Results on Reinforced Concrete Shear Walls and Analysis on Them*, in Japanese, Building Research Institute, Ministry of Construction of Japan, Mar., 1975.
16. Hwang, T-H., "Effects of Variation in Load History on Cyclic Response of Concrete Flexural Members," presented to the University of Illinois, at Urbana, Ill., in 1982, in partial fulfillment of the requirements for the degree of Doctor of Philosophy.
17. Jirsa, J. O., and Marques, J. L. G., "A Study of Hooked Bar Anchorage in Beam-Column Joints," *Report to Reinforced Concrete Research Council (Project 33)*, University of Texas, Austin, Tex., July, 1972.
18. Kani, G. N. J., "The Riddle of Shear Failure and Its Solution," *Journal of ACI*, Apr., 1964.
19. Kent, D. C., and Park, R., "Flexural Members with Confined Concrete," *Journal of the Structural Engineering Division*, ASCE, Vol. 97, No. ST7, July, 1971.
20. Koike, K., Takeda, J., Yoshioka, K., and Nakayama, T., "On the Yield Deformation of Reinforced Concrete Columns," in Japanese, *Annual Conference of AIJ*, Oct., 1974.

J. Struct. Eng. 1985.111:722-739.

21. Küstü, O., and Bouwkamp, J. G., "Behavior of Reinforced Concrete Deep Beam-Column Subassemblages Under Cyclic Loads," University of California, at Berkeley, EERC, *Report No. 73-8*, Berkeley, Calif., May, 1975.
22. Ma, S.-Y., M., Bertero, V. V., and Popov, E. P., "Experimental and Analytical Studies on the Hysteretic Behavior of Reinforced Concrete Rectangular and t-Beams," University of California at Berkeley, EERC, *Report No. 76-2*, Berkeley, Calif., May, 1976.
23. McCollister, H. M., Siess, C. P., and Newmark, N. M., "Load-Deformation Characteristics of Simulated Beam-Column Connection in Reinforced Concrete," *Civil Engineering Studies*, Structural Research Series No. 76, University of Illinois, Urbana, Ill., June, 1954.
24. Morita, S., and Tomita, K., "Basic Study on Bond Between Steel and Concrete," in Japanese, *Transactions*, Architectural Institute of Japan, Jan., 1967; Feb., 1967; Mar., 1967; and Sept., 1967.
25. Morita, S., Sumi, T., and Kiguchi, S., "Bond Behavior of Reinforcing Bars in Anchorage Under Cyclic Loading," in Japanese, *Annual Conference of AIJ*, Oct., 1975.
26. NewMark, N. M., Siess, C. P., and Sozen, M. A., "Moment-Rotation Characteristics of Reinforced Concrete and Ductility Requirement for Earthquake Resistance," *Proceedings, 30th Annual Convention of SEAOC*, 1963.
27. Olesen, S. O., Sozen, M. A., and Siess, C. P., "Investigation of Prestressed Reinforced Concrete for Highway Bridges; Part IV: Strength in Shear of Beams with Web Reinforcement," Engineering Experiment Station, *Bulletin 493*, University of Illinois, Urbana, Ill., July, 1967.
28. Park, R., and Paulay, T., *Reinforced Concrete Structures*, John Wiley and Sons, Inc., New York, N.Y., 1974.
29. Park, Y.-J., Ang, A. H.-S., and Wen, Y. K., "Seismic Damage Analysis of Reinforced Concrete Buildings," *Journal of Structural Engineering*, ASCE, Vol. 111, No. 4, Apr., 1985, pp. 740–757.
30. Umemura, H., and Takizawa, H., "Dynamic Response of Reinforced Concrete Buildings," *Structural Engineering Documents*, IABSE, 1982.
31. Wight, J. K., and Sozen, M. A., "Shear Strength Decay in Reinforced Concrete Columns Subjected to Large Deformatin Reversals," Civil Engineering Studies, *Structural Research Series No. 403*, University of Illinois, Urbana, Ill., Aug., 1973.

APPENDIX II.—NOTATION

The following symbols are used in this paper:

A = area of longitudinal reinforcing bar;
a = height of the compression stress block;
a_c = area of compression reinforcement;
a_t = area of tension reinforcement;
b = width of cross section;
D = damage index, or diameter of main reinforcement;
d = effective height of cross section, or diameter of stirrup;
d_c = distance from extreme compression fiber to centroid of compression reinforcement;
dE = incremental absorbed hysteretic energy;
$E_c(\delta)$ = hysteretic energy per cycle at deformation δ;
E_S = modulus of elasticity of steel;
f'_c = compressive strength of concrete;
h = height of cross section;
l = length of member;
l' = length of "no shear cracking zone";

l_i = arm length measured from the end of shear cracking;
M_c = cracking moment;
M_y = yield moment;
N = axial force;
n_o = normalized axial stress;
p_t = tension steel ratio;
p_w = stirrup ratio;
Q_c, Q_y, Q_u = cracking, yield, maximum shear strength, respectively;
S = bond slippage;
S_n = normalized slippage from anchorage;
Z = distance from centroid of tension reinforcement to compression reinforcement;
α, β = constant values in damage index;
$\delta_f, \delta_b, \delta_s, \delta_e$ = flexural, bond slippage, inelastic shear, elastic shear deformation at yielding, respectively;
δ_M = maximum deformation sustained by member;
δ_y = yield deformation;
δ_u = ultimate deformation under static loading;
ϵ_b = flexural concrete strain at location of compression reinforcing bar;
ϵ_o = compressive strain of concrete at maximum stress;
ϵ_p = maximum principal strain of concrete at yielding;
ϵ_y = yield strain of steel;
θ_s = shear rotation;
μ = ductility factor;
μ_u = ultimate ductility factor;
ρ_w = confinement ratio;
σ_o = stress of reinforcing bar at face of anchorage;
τ = bond stress;
τ_B = effective average bond stress;
τ_M = maximum bond stress;
ϕ_y = yield curvature; and
ψ = perimeter of longitudinal reinforcing bar.